Activity-dependent neural network model on scale-free networks

Gian Luca Pellegrini,[1] Lucilla de Arcangelis,[2] Hans J. Herrmann,[3] and Carla Perrone-Capano[4,5]
[1]*Department of Physical Sciences, University of Naples Federico II, 80125 Napoli, Italy*
[2]*Department of Information Engineering and CNISM, Second University of Naples, 81031 Aversa (CE), Italy*
[3]*Computational Physics, IfB, ETH-Hönggerberg, Schafmattstrasse 6, 8093 Zürich, Switzerland*
[4]*Department of Biological Sciences, University of Naples "Federico II", 80134, Naples, Italy*
[5]*IGB "A.Buzzati Traverso," CNR, 80131 Naples, Italy*
(Received 23 October 2006; published 17 July 2007)

Networks of living neurons exhibit an avalanche mode of activity, experimentally found in organotypic cultures. Moreover, experimental studies of morphology indicate that neurons develop a network of small-world-like connections, with the possibility of a very high connectivity degree. Here we study a recent model based on self-organized criticality, which consists of an electrical network with threshold firing and activity-dependent synapse strengths. We study the model on a scale-free network, the Apollonian network. The system exhibits an avalanche activity with a power law distribution of sizes and durations. The analysis of the power spectra of the electrical signal reproduces very robustly the power law behavior with the exponent 0.8, experimentally measured in electroencephalogram spectra. The exponents are found to be quite stable with respect to initial configurations and strength of plastic remodeling, indicating that universality holds for a wide class of neural network models.

DOI: 10.1103/PhysRevE.76.016107 PACS number(s): 05.65.+b, 87.19.La, 05.45.Tp, 89.75.−k

I. INTRODUCTION

Neuronal networks [1] exhibit diverse patterns of activity, including oscillations, synchronization, and waves. During neuronal activity, each neuron can receive inputs from thousands of other neurons and, when it reaches a threshold, redistributes this integrated activity back to the neuronal network. Recently a neuronal activity based on avalanches has been observed in organotypic cultures from coronal slices of rat cortex [2] where neuronal avalanches are stable for many hours [3]. More precisely, recording spontaneous local field potentials continuously with a multielectrode array has shown that activity initiated at one electrode might spread to other electrodes not necessarily contiguously, as in a wavelike propagation. Cortical slices are then found to exhibit a new form of activity, producing several thousand avalanches per hour of different duration, in which nonsynchronous activity is spread over space and time. By analyzing the sizes and durations of neuronal avalanches, the probability distribution reveals a power law behavior, suggesting that the cortical network operates in a critical state. The experimental data indicate for the avalanche size distribution a slope varying between −1.2 and −1.9, depending on the accuracy of the time-binning procedure, with a value −1.5 for optimal experimental conditions. Interestingly, the power law behavior is destroyed when the excitability of the system is increased, contrary to what expected, since the incidence of large avalanches should decrease the power law exponent. The distribution then becomes bimodal—i.e., dominated by either very small or very large avalanches as in epileptic tissues. The power law behavior is therefore the indication of an optimal excitability in the systems spontaneous activity. Moreover, the avalanche time duration is also found to follow a power law behavior as a function of the duration time, normalized by the time bin, with an exponent equal to −2.0 followed by an exponential cutoff. These results have been interpreted relating spontaneous activity in a cortical network to a critical branching process [4,5]. Indeed the experimental branching parameter is found to be very close to the critical value equal to 1, at which avalanches at all scales exist.

Power law behavior is also observed for other neurobiological systems at various levels, such as, for instance, in power spectra of different time series monitoring neuronal activities. Prominent examples are electroencephalogram (EEG) data which are used by neurologists to discern sleep phases and diagnose epilepsy and other seizure disorders as well as neuronal network damage and disease [6,7]. The interpretation of physiological mechanisms at the basis of EEG measurements is still controversial. The medical analysis is usually performed by measuring the frequency position of a number of peaks in the spectrum, which usually appear on an underlying power law behaviour. Another example of a physiological function which can be monitored by time series analysis is the human gait, which is controlled by the brain [8]. For all these time series the power spectrum—i.e., the square of the amplitude of the Fourier transform, double logarithmically plotted against frequency—generally features a power law over at least one or two orders of magnitude with exponents between 1 and 0.7. Moreover, experimental results show that the neurotransmitter secretion rate exhibits fluctuations in time having power law behavior [9] and power laws are also observed in fluctuations of extended excitable systems driven by stochastic fluctuations [10].

The dynamics observed in spontaneous neuronal network activity is very similar to self-organized criticality (SOC) [11–14]. The term SOC usually refers to a mechanism of slow energy accumulation and fast energy redistribution, driving the system toward a critical state, where the distribution of avalanche sizes is a power law obtained without fine-tuning: no tunable parameter is present in the model. The simplicity of the mechanism at the basis of SOC has suggested that several phenomena characterized by power law in the size distribution represent natural realizations of SOC.

For instance, SOC has been proposed to model earthquakes [15–17], the evolution of biological systems [18], solar flare occurrence [19], fluctuations in confined plasma [20], snow avalanches [21], and rainfall [22].

On the basis of these observations, recently a model based on SOC ideas and taking into account synaptic plasticity in a neural network [23] has been proposed. Plasticity is one of the most astonishing properties of the neuronal network, occurring mostly during development and learning [24–26], and can be defined as the ability to modify the structural and functional properties of synapses. Among the mechanisms for synaptic plasticity, the activity-dependent Hebbian plasticity constitutes the most fully developed and influential model of how information is stored in neuronal circuits [27–29]. Within the present SOC approach the four most important ingredients for neuronal activity have been introduced: namely threshold firing, neuron refractory period, activity-dependent synaptic plasticity, and pruning.

The model consists in a network of sites, which represent the cell body of a neuron, and bonds, which constitute the synapses connecting different neurons. For the sake of simplicity, the model is implemented on a square lattice. In order to study the electrical activity of the network, each site is characterized by a potential and each bond by a conductance. Whenever, at a given time, the value of the potential at a site is above a certain threshold, approximately equal to −55 mV for real neurons, the neuron fires—i.e., generates an "action potential"—distributing charges to its connected neighbors in proportion to the current flowing through each bond. After firing, a neuron goes back to the resting potential of −70 mV and remains inactive during the so-called refractory period. This time corresponds for real neurons to the physiological time needed to reset ion channels after the transmission of the action potential through the axon. The conductances, on the other hand, represent Hebbian synapses, for which the conjunction of activity at the presynaptic and post-synaptic neurons modulates the efficiency of the synapse [29]. To this extent, each time a synapse transmits an action potential between active neurons, its strength is increased proportionally to the intensity of the transmitted signal, whereas synapses inactive during a neuronal avalanche have their strength decreased, as for Hebbian rules. Synapses successively weakened may have their strength finally set to zero—i.e., are "pruned"—eliminating that particular connection between neurons. Pruning implies that, as activity goes on, the initial regular lattice is transformed, some patterns are strengthened, some are weakened, and the connectivity degree of some neurons may be decreased. The system is found to exhibit an avalanche activity power law distributed with an exponent close to −1.5, as measured for spontaneous activity size distribution [2]. The analysis of the power spectra of the electrical signal reproduces very robustly the power law behavior with the exponent 0.8, experimentally measured in EEG spectra. The same value of both exponents is found considering leaky neurons or introducing a small percentage of inhibitory synapses, indicating that universality holds for a wide class of neural network models.

In real neuronal networks, neurons are known to be able to develop an extremely high number of connections with other neurons; that is, a single-cell body may receive inputs from even 1000 presynaptic neurons. One of the most fascinating questions is how an ensemble of living neurons self-organizes, developing connections to give origin to a highly complex system. The dynamics underlying this process should be driven both by the aim of realizing a well-connected network leading to efficient information transmission and the energetic cost of establishing very long connections. The morphological characterization of a neuronal network grown *in vitro* has been studied [30] by monitoring the development of neurites in an ensemble of few hundreds neurons from the frontal ganglion of adult locusts. After few days the cultured neurons have developed an elaborated network with hundreds of connections, whose morphology and topology have been analyzed by a mapping onto a connected graph. The short path length and the high clustering coefficient measured indicate that the network belongs to the category of small-world networks [31]. Small-world networks are characterized by an efficient information transmission with a small number of long-range connections. However, the system grown *in vitro* necessarily lacks some features of *in vivo* systems; therefore, the average node connectivity is found equal only to few units and the "scale-free" feature [32] of many real networks was not recovered. Further recent experimental [33] and theoretical [34] investigations have confirmed that neuronal networks have complex connection properties. In particular, Roerig *et al.* have found, combining *in vitro* and *in vivo* techniques, that in the visual cortex V1 of ferrets the dependence of the number of connections to a central neuron on the distance has a power law behavior: the central neuron makes a large number (up to 1000) of short connections (few micrometers) and a few long-range connections (some millimeters). This result characterizes fractally coupled networks, which indeed have small-world properties and high clustering coefficient.

The activity-dependent neural network model [23] has been implemented on small-world networks by rewiring a small percentage of the square lattice bonds. Again the same universal scaling behavior is recovered on small-world networks for both the avalanche distribution and the power spectra. The simple rewiring procedure, however, only allows long-range connections, leaving the average node connectivity equal to a few units, as for *in vitro* systems. It would be interesting to investigate the case of a wider range of connectivity degrees, as observed for neuronal networks.

In this paper we investigate the behavior of the activity-dependent neural network model on scale-free networks. These are indeed characterized by a power law distribution of the node connectivity, allowing a high number of connections per neuron. We develop the model on the Apollonian network [35], which has the property of being simultaneously small world and scale free. We analyze the behavior of the avalanche size and duration distributions and the power spectra related to electrical activity. We also study a system composed of both excitatory and inhibitory synapses, as in real neuronal networks. The paper is organized as follows: In Sec. II the scale-free Apollonian network is described, whereas in Sec. III the activity-dependent neural network model is presented and the results on the electrical activity are discussed in Sec. IV. Concluding remarks are given in Sec. V.

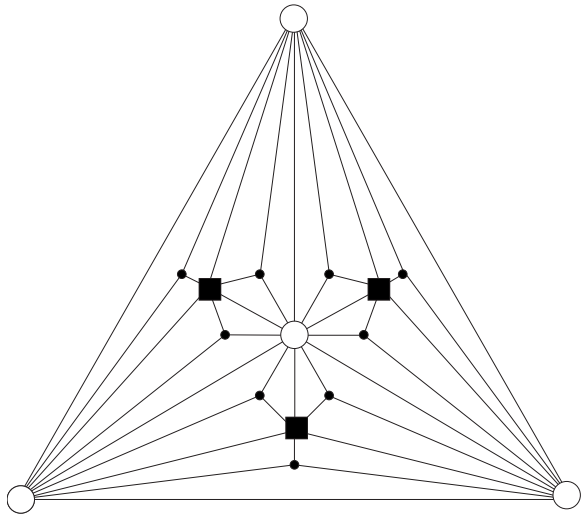

FIG. 1. Apollonian network for $N=2$: iterations $n=0,1,2$ are symbols ○, ■, •, respectively.

II. APOLLONIAN NETWORK

The Apollonian network has been recently introduced [35] in a simple deterministic version starting from the problem of space-filling packing of spheres according to the ancient Greek mathematician Apollonius of Perga. In its classical version the network associated to the packing gives a triangulation that physically corresponds to the force network of the packing. One starts with the zeroth-order triangle of corners P_1,P_2,P_3, places a fourth site P_4 in the center of the triangle, and connects it to the three corners ($n=0$). This operation will divide the original triangle in three smaller ones, having in common the central site. The iteration $n=1$ proceeds placing one more site in the centre of each small triangle and connecting it to the corners (Fig. 1). At each iteration n, going from 0 to N, the number of sites increases by a factor of 3 and the coordination of each already existing site by a factor of 2. More precisely, at generation N there are

$$m(k,N) = 3^N, 3^{N-1}, 3^{N-2}, \ldots, 3^2, 3, 1, 3$$

vertices, with connectivity degree

$$k(N) = 3, 3\times 2, 3\times 2^2, \ldots, 3\times 2^{N-1}, 3\times 2^N, 2^{N+1}+1,$$

respectively, where the two last values correspond to the site P_4 and the three corners P_1,P_2,P_3. The maximum connectivity value then is the one of the very central site P_4, $k_{max}=3\times 2^N$, whereas the sites inserted at the Nth iteration will have the lowest connectivity 3.

The important property of the Apollonian network is that it is scale free. In fact, it has been shown [35] that the cumulative distribution of connectivity degrees $P(k)=\Sigma_{k'\geq k} m(k,N)/N_N$, where $N_N=3+(3^{(N+1)}-1)/2$ is the total number of sites at generation N, has a power law behavior with k. More precisely, $P(k)\propto k^{1-\gamma}$, with $\gamma=\ln 3/\ln 2 \sim 1.585$. Moreover, the network has small-world features. This implies [31] that the average length of the shortest path l behaves as in random networks and grows slower than any positive power of N—i.e., $l\propto(\ln N)^{3/4}$. Furthermore, the clustering coefficient C is very high as in regular networks ($C=1$) and contrary to random networks. For the Apollonian network C has been found to be equal to 0.828 in the limit of large N. On this basis, the Apollonian network appears to have all the new features that we would like to investigate: small-world property found experimentally [30] and possibility of a very high connectivity degree (scale free). Moreover, it also presents site-connecting bonds of all lengths. Also this last feature can be found in real neuronal networks, where the length of an axon connecting the presynaptic with the post-synaptic neuron can vary over several orders of magnitude, from micrometers to centimeters.

III. ACTIVITY-DEPENDENT MODEL

On a Apollonian network at generation N, we assign at each site a neuron at potential v_i and at each bond a synapse of conductance g_{ij}. Since a neuron receives inputs on the dendrites and sends signals through the axon, bonds are asymmetric and therefore $g_{ij}\neq g_{ji}$. Whenever at time t the value of the potential at a site i is above a certain threshold, $v_i\geq v_c$, the neuron generates an action potential, distributing charges to connected neurons j in proportion to the current flowing through each bond:

$$v_j(t+1) = v_j(t) \pm v_i(t)\frac{i_{ij}(t)}{\sum_k i_{ik}(t)}, \tag{1}$$

where $v_j(t)$ is the potential at time t of site j, connected to site i, $i_{ij}=g_{ij}(v_i-v_j)$, and the sum is extended to all k sites connected to site i, at a potential $v_k<v_i$. In mature living neuronal circuits, synapses can be excitatory or inhibitory; namely, they set the potential of the post-synaptic membrane to a level, respectively, closer to or farther from the firing threshold. This ingredient can be introduced by considering each synapse inhibitory with probability p_{in} and excitatory with probability $1-p_{in}$. In Eq. (1) the plus sign corresponds to an excitatory synapse, whereas the minus sign to an inhibitory one. After firing, a neuron is set to a zero resting potential. Equation (1) intends to simplify the very complex neuronal signal transmission, taking into account the observed behavior that different post-synaptic neurons may receive signals of different intensity from the same presynaptic neuron.

The conductances can be initially set all equal or else random between 0 and 1, whereas the neuron potentials are uniformly distributed random numbers between v_c-2 and v_c-1. In agreement with the SOC scenario, the initial state for the voltage is not relevant since the system evolves toward the same critical state regardless of the initial condition. The potential is fixed to zero at the three corner sites 1,2,3 where information can flow out of the system. The external stimulus is imposed at one input site chosen either fixed or random.

The firing rate of real neurons is limited by the refractory period—i.e., the brief period after the generation of an action potential during which a second action potential is difficult or impossible to elicit. The practical implication of refractory periods is that the action potential does not propagate back

toward the initiation point and therefore is not allowed to reverberate between the cell body and the synapse. In the model, once a neuron fires, it remains quiescent for one time step and is therefore unable to accept charge from firing connected neurons. This ingredient indeed turns out to be crucial for a controlled functioning of the numerical model. In this way an avalanche of charges can propagate far from the input site through the system.

As soon as a site is at or above threshold, v_c, at a given time t, it fires according to Eq. (1). Then the conductance of all the bonds, connecting active neurons and that have carried a current, is increased in the following way:

$$g_{ij}(t+1) = g_{ij}(t) + \delta g_{ij}(t), \tag{2}$$

where $\delta g_{ij}(t) = A\alpha i_{ij}(t)$, with α being a dimensionless parameter and A a unit constant bearing the dimension of an inverse potential. After applying Eq. (2), the time variable of the simulation is increased by one unit. Equation (2) describes the mechanism of increase of synaptic strength, tuned by the parameter α. This parameter then represents the ensemble of all possible physiological factors influencing synaptic plasticity, many of which are not yet fully understood.

Once an avalanche of firings comes to an end, the conductance of all the bonds with nonzero conductance is reduced by the average conductance increase per bond during that avalanche, $\Delta g = \Sigma_{ij,t} \delta g_{ij}(t)/N_b$, where N_b is the number of bonds with nonzero conductance. This weakening rule implies the conservation of the average bond conductance. This requirement is necessary in our numerical network in order to keep the total current flowing in the system finite and therefore needs to be applied at the end of each avalanche. The quantity Δg depends on α and on the response of the neural network to a given stimulus. Once the conductance of a bond is below an assigned small value σ_t, it is removed—i.e., is set equal to zero, which corresponds to what is known as pruning. It is important to notice that, since the conductance network is one-directional, pruning may eliminate the connection going from neuron i to neuron j and not the one in the opposite direction. In this way the network "memorizes" the most used paths of discharge by increasing their conductance, whereas the less used synapses atrophy. This remodeling of synapses mimics the fine-tuning of wiring that occurs in developing neuronal networks, when neuronal activity can modify the synaptic circuitry, once the basic patterns of neuronal network wiring are established [25]. These mechanisms correspond to a Hebbian form of activity-dependent plasticity, where the conjunction of activity at the presynaptic and post-synaptic neuron modulates the efficiency of the synapse [29]. To ensure the stable functioning of neural circuits, both strengthening and weakening rules of Hebbian synapses are necessary to avoid instabilities due to positive feedback [36]. However, differently from the well-known long-term potentiation (LTP) and long-term depression (LTD) mechanisms [1], the modulation of synaptic strengths does not depend on the frequency of synapse activation [24,37,38].

The external driving mechanism to the system is imposed by setting the potential of the input site to the value v_c, corresponding to one stimulus. This external stimulus is needed to keep the system "alive." The discharge evolves until no further firing occurs; then, the next stimulus is applied. Our model therefore does not describe the real evolution in time but only the sequence of events on the artificial time scale imposed by the propagation of the signals, which are discrete by nature.

IV. NUMERICAL RESULTS

We consider an Apollonian net at the generation $N=9$ (29 527 neurons and 177 150 synapses). The three corner sites of the system have always zero potential and represent open boundaries. The input site is either chosen at random or fixed. Synapses can be excitatory or inhibitory with probability p_{inh}. Initial conductances are assigned either all equal to $g_0=0.25$ or randomly distributed between 0 and 1. The other parameters in the simulation are the firing threshold $v_c=6$ and the conductance cutoff for pruning $\sigma_t=0.0001$. Their value does not influence the simulation results. In the first three subsections, we consider a network composed exclusively by excitatory synapses. In the last subsection, we investigate the dependence of the results on the percentage of inhibitory synapses.

A. Pruning

The strength of the parameter α, controlling both the increase and decrease of synaptic strengths, determines the plasticity dynamics in the network. In fact, the more the system learns, strengthening the used synapses, the more the unused connections will weaken. We apply a sequence of external stimuli and we measure the total number of pruned bonds at the end of each avalanche, N_{pb}. This quantity in general could depend on the initial conductance g_0; therefore, the two cases of all initial conductances equal to 0.25, and uniformly distributed between 0 and 1, are investigated.

First the case of equal initial conductances is analyzed. For each value of α the average number of pruned bonds, N_{pb}, is monitored as function of the number of applied external stimuli. For input sites randomly chosen at each stimulus, Fig. 2 shows that pruning starts after applying a certain number of stimuli, since all conductances are initially equal to 0.25 and N_{pb} increases more rapidly with N_p for larger α. The plateau is reached after about 2000 stimuli (for every α) after which N_{pb} increases only of few units in time. From the asymptotic value of each curve we can evaluate the asymptotic number of active bonds as the difference of the total number of bonds minus the asymptotic value of N_{pb}. We plot it as function of α and determine that the value of α maximizing the number of active bonds is about 0.020. This could be interpreted as an optimal value for the system with respect to plastic adaptation: it maximizes the number of active connections under the competing strengthening and weakening rules.

In order to understand if pruning acts in the same way on bonds created at different iterations n, $n=0,\ldots,N$, or rather tends to eliminate bonds of some particular iteration, the probability to prune bonds of different n is evaluated—that is, the number of pruned bonds over the total number of

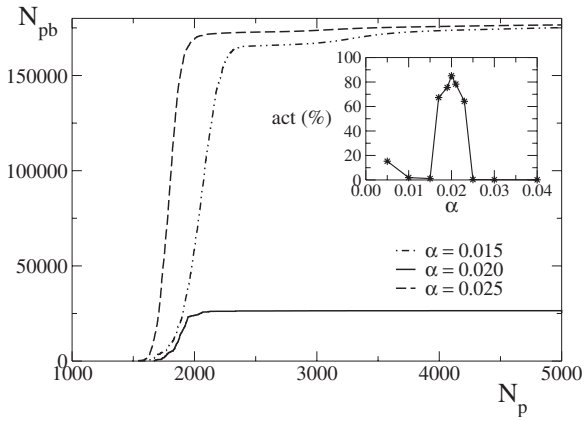

FIG. 2. Average number of pruned bonds as function of the number of external stimuli, N_p, for three different values of α and equal initial conductances. In the inset, the percentage of the asymptotic number of active bonds as function of α. The maximum is for α=0.020, where are active about 80% of bonds.

bonds for each iteration stage—as a function of the number of applied stimuli. Figure 3 shows that the plateau is reached at about the same value of N_p and the shape of the curve is similar for each n. However, the probability to prune bonds with large n is higher: These are the bonds created in the last iterations and therefore embedded in the interior of the network. This suggests that the most active bonds are the long-range ones (small n), which therefore support most of the information transport through the network. In the inset of Fig. 3 we show the asymptotic number of pruned bonds per generation on a semilogorithmic scale; this quantity is well fitted by the exponential behavior $N_{pb} \simeq \exp n$.

The same analysis has been performed for random initial conductances between 0 and 1. The results are similar to the previous case. It can be noticed that pruning starts already at N_p=1, since conductances close to zero are present, and the plateau is reached after about 1000 stimuli. The value of α which now optimizes the number of active bonds is about 0.030. Finally the pruning behavior for different iterations is

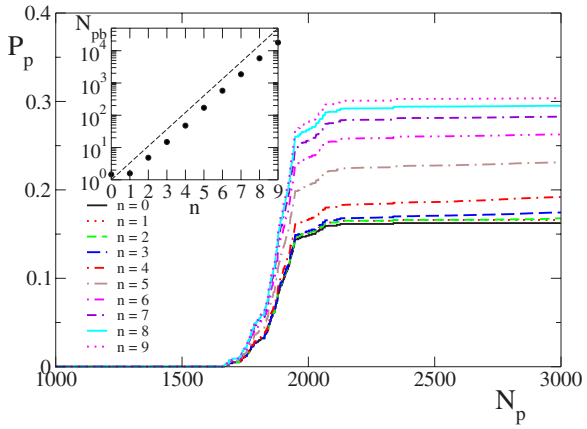

FIG. 3. (Color online) Probability of pruning for bonds of different iterations n, from bottom n=0 to top n=9, as a function of the number of external stimuli, N_p, for equal initial conductances. In the inset, the asymptotic N_{pb} (after 5000 stimuli) as a function of n with the exponential fit $N_{pb} \simeq \exp 1.2n$.

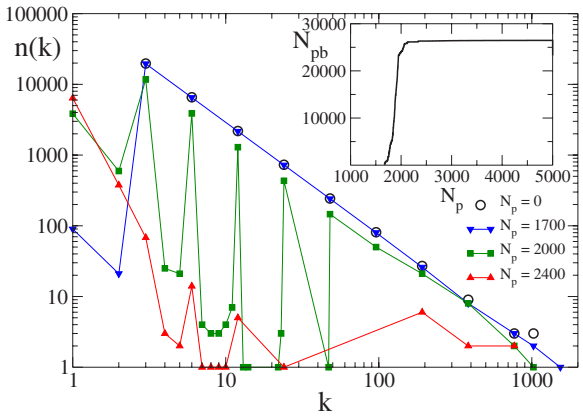

FIG. 4. (Color online) Connectivity degree distribution $n(k)$ at different pruning stages N_p for equal initial conductances and α =0.020. As soon as pruning starts to eliminate bonds, new connectivity degrees appear, not present in the original network. For instance one of the three-corner sites, which for the generation N=9 has initially a connectivity degree 1025, may lose one bond because of pruning. As a result, $n(1025)$=2 and the new degree value 1024 appears in the distribution $n(k)$. In the inset, the corresponding behavior of the number of pruned bonds.

similar to the previous case, with the pruning probability exponentially increasing with n, as $N_{pb} \simeq \exp n$.

The effect of pruning on the connectivity degree of the network (Fig. 4) has also been analyzed. We evaluate the number of sites with a number of outgoing connections k as function of k in the initial network and after application of a given number of external stimuli. For each neuron, k represents the number of connected post-synaptic neurons. In order to identify the different stages in the pruning process, the inset of Fig. 4 shows the total number of pruned bonds as function of N_p. After the application of few external stimuli—i.e., for a short plastic training—the distribution $n(k)$ shows the same scaling behavior of the Apollonian network. As the pruning process goes on, sites vary their connectivity degree and new values of k appear. The result is that the scaling behavior is progressively lost, as well as the scale-free character of the network, since there is a generalized decrease of the connectivity in the network.

B. Avalanche distributions

After training the system applying plasticity rules during N_p external stimuli, we submit the system to a new sequence of stimuli with no modification of synapse strengths. The response of the system to this second sequence models the activity of a trained neuronal network with a given level of experience. We analyze this response by measuring the avalanche size distribution $n(s)$, the time duration distribution $n(T)$, and the power spectrum $S(f)$.

The avalanche size distribution $n(s)$ consistently exhibits power law behavior for different values of model parameters. Figure 5 shows the avalanche size distribution for different values of N_p, including also the case N_p=0 (no plasticity training), for random initial conductances and the optimal value of α=0.030. We notice that, for fixed size s, increasing

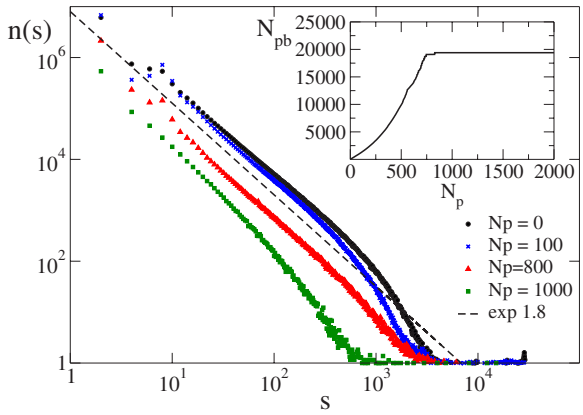

FIG. 5. (Color online) Avalanche size distribution for different values of N_p, random initial conductances, $\alpha=0.030$, and random input site. Data are logarithmically binned. In the inset, the corresponding behavior of the number of pruned bonds.

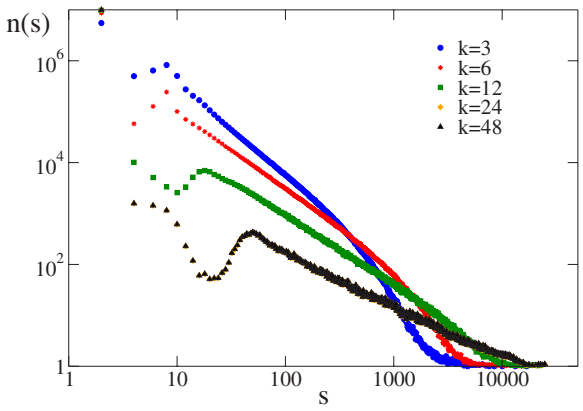

FIG. 6. (Color online) Avalanche size distribution for input sites randomly chosen among sites with the same connectivity degree k. Data are logarithmically binned. Only distributions for small k are shown; for higher k, the scaling behavior is lost (random initial conductances, $\alpha=0.030$, $N_p=100$).

N_p decreases the number of avalanches of that size, suggesting that strong plasticity remodeling decreases activity. The exponent appears to be independent of N_p, as long as the number of pruned bonds, N_{pb}, is far from the plateau (see inset in Fig. 5). Similar results are found for equal initial conductances. The value of the exponent is $\sigma=1.8\pm0.2$ and is stable with respect to variations of the parameter α for both equal and random initial conductances. This value is compatible within error bars with the value found in the experiments of Beggs and Plentz [2], 1.5 ± 0.4, and with previous results of the model on both regular and small-world lattices. However, one has to notice that experimental results for neuronal avalanches were obtained for local field potentials; i.e., the underlying events correspond to local population spikes, whereas the numerical events are single neuronal spikes. The slightly larger value of the exponent, found on the Apollonian network, suggests that the high level of connectivity reduces the probability of very large avalanches but does not change substantially the electrical activity behaviour. For largerN_p, the distribution exhibits an increase in the scaling exponent and finally loses the scaling behavior for very large N_p values, in the plateau regime for the number of pruned bonds.

It is important to investigate the role of the choice of the fixed input site, since in the Apollonian network, contrary to the regular network, sites have very different connectivity degrees. Figure 6 shows the avalanche size distribution for fixed input sites chosen among sites with given connectivity degree k. In this way it is possible to detect solely the effect due to the connectivity of the input site, eliminating all other effects due to the particular position of the input site in the network. Power law behavior is found for connectivity degrees of the input site up to $k=12$. The scaling exponent decreases with increasing input site connectivity degree k; that is, for larger k larger avalanches become more probable. However, if the connectivity degree increases above 12, the scaling behavior is lost. This is due to the fact that an input site with very high connectivity must distribute its charge to many connected sites and therefore the network activity will be damped already at the initial stage. Therefore, to reproduce the experimentally observed scaling behavior, the fixed input site should be chosen with low connectivity degree ($k\leq12$). The avalanche size distribution for fixed input site, with connectivity $k=3$ or $k=6$, exhibits power law behavior with the same exponents found for random input site: $\sigma=1.8\pm0.2$ for equal and random initial conductances.

At time $t=0$ a neuron is activated by an external stimulus initiating the avalanche. This will continue until no neuron is at or above threshold. The number of avalanches lasting a time T, $n(T)$, as a function of T exhibits power law behavior (Fig. 7) with an exponential cutoff. The scaling exponent is found to be $\tau=2.1\pm0.2$ for equal and random initial conductances. This value is found to be stable with respect to different α (Fig. 7) and N_p, provided that the number of pruned bonds, N_{pb}, is lower than the plateau for that value of α. Moreover, it does not depend on the choice of the input site, either fixed or random. Finally both values agree within error bars with the value 2.0, the exponent found experimentally by Beggs and Plentz [2].

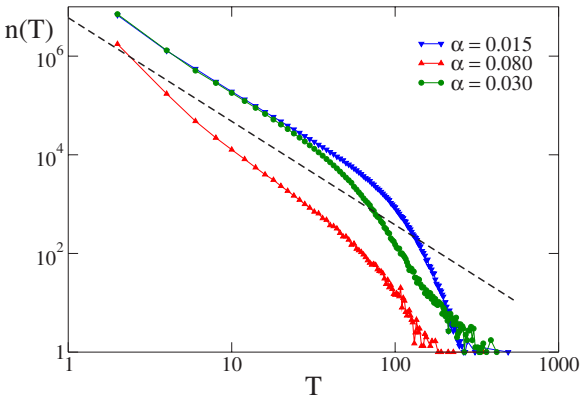

FIG. 7. (Color online) Avalanche duration distribution for different values of α (random initial conductances, random input sites, $N_p=500$). Data are logarithmically binned. The dotted line has slope 2.1.

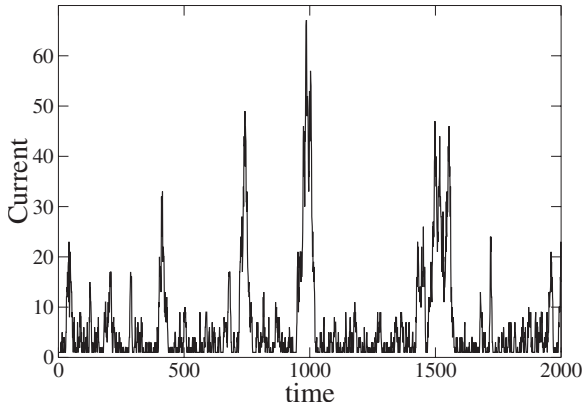

FIG. 8. Total current flowing in the system as function of time. Avalanches of all sizes can be observed.

C. Power spectra for electrical activity

The power spectrum of the time signal for the overall electrical activity can be calculated. The aim is to compare the scaling behavior of the numerical spectrum with the power law observed usually in medical data [39,40]. For this purpose, the number of active neurons is monitored as function of time for random external stimuli, which recalls the experimental condition in which electrodes are placed on the scalp in order to study neuronal network spontaneous electrical activity. Figure 8 shows an example of neuronal activity where avalanches of all sizes can be generated in response to the external stimulus. Here the unit time is the time for the avalanche to propagate from one neuron to the connected one. The power spectrum is calculated as the squared amplitude of the time Fourier transform as a function of frequency, averaged over many initial configurations. Because of the definition of the numerical time unit, the frequency unit does not correspond to the experimental one in hertz.

Figure 9 shows the spectrum for equal initial conductances and different values of N_p. For $N_p=0$—i.e., when no plasticity mechanism is applied—the spectrum has a behavior $1/f$, characteristic of SOC. For values of N_p different from zero, but before the N_{pb} plateau, one can distinguish two different regimes: a power law behavior with exponent $\beta=0.8\pm0.1$ at high frequency, followed by a crossover toward white noise at low frequency. However, for $N_p=2000$ (close to the plateau value for N_{pb}) the scaling behavior with exponent 0.8 is detected over a wider frequency range. The difference between $\beta=1$ for $N_p=0$ and $\beta\simeq0.8$ for higher N_p suggests that plasticity reduces the power spectrum exponent, in better agreement with experimental EEG spectra [39,40]. The stability of the exponent with respect to α has also been verified, finding consistently $\beta=0.8\pm0.1$ at high frequency. Finally the power spectrum for fixed input site shows a scaling exponent $\beta=0.8\pm0.1$ over two orders of magnitude. The measured value for the power spectra exponent is in agreement with the expected relation $\beta=3-\tau$, being the scaling exponent of the avalanche duration distribution, $-\tau<-1$ [12].

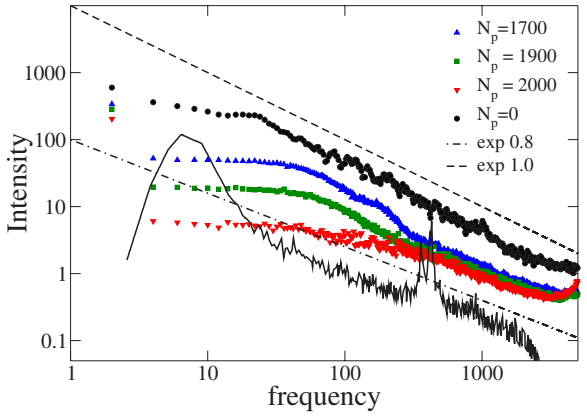

FIG. 9. (Color online) Power spectra obtained for different N_p, equal initial conductances, $\alpha=0.020$, and random input sites. The experimental data (black line) are from Ref. [40] with frequency in Hz. Experimental data are shifted in order to be in the same frequency range of numerical data.

The scaling behavior of the power spectrum can be interpreted in terms of a stochastic process determined by multiple random inputs [41]. In fact, the output signal resulting from different and uncorrelated superimposed processes is characterized by a power spectrum with power law behavior and a crossover to white noise at low frequencies. The crossover frequency is related to the inverse of the longest characteristic time among the superimposed processes. The value of the scaling exponent depends on the ratio of the relative effect (signal amplitude) on the output of a process of given frequency with respect to processes with a different frequency. $1/f$ noise corresponds to a superposition of processes of different frequencies, all having the same amplitude. In our case the scaling exponent is smaller than unity, suggesting that processes with high characteristic frequency are more relevant than processes with low frequency in the superposition [41].

D. Inhibitory synapses

We have investigated the dependence of the previous results on the probability p_{in}, for a synapse to be inhibitory. The avalanche size and duration distributions show that the exponents σ and τ increase for increasing p_{in}; therefore, for a high percentage of inhibitory synapses the probability of large avalanches decreases (Fig. 10). On the regular lattice for $p_{in}=0.5$ no longer power law but exponential behavior is found [23]. In the present case scaling behavior persists, due to the very high connectivity degree.

The power spectra for different values of p_{in} exhibit a complex behavior. In fact, for a small fraction of inhibitory synapses ($p_{in}\leq0.05$), the power law exponent β increases with respect to the case where synapses are all excitatory, up to a value 1.2. Then, for $p_{in}\sim0.10$, the exponent decreases toward values compatible with experimental results—i.e., between 0.7 and 1.0. By increasing further the percentage of inhibitory synapses, to values close or greater than 0.2, the spectrum becomes the white noise one.

V. CONCLUSIONS

Extensive simulations have been performed for the activity-dependent neural network model implemented on

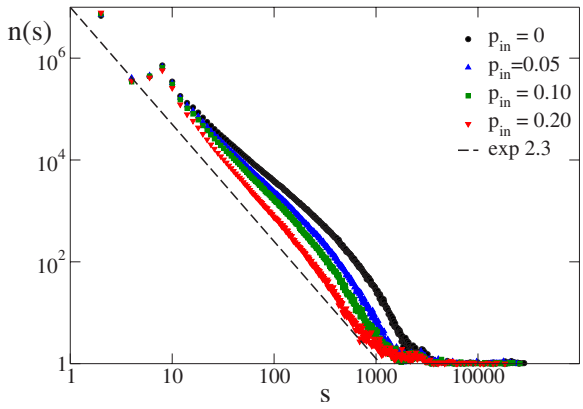

FIG. 10. (Color online) Avalanche size distributions for different p_{in}, equal initial conductances, α=0.020, random input sites, and N_p=1700. Data are logarithmically binned.

the scale-free Apollonian network. The results are compared with previous simulations on regular and small-world lattices and with experimental data. We first find that an optimal value of the plasticity strength α exists with respect to the pruning process: this value maximizes the number of active connections under the competing strengthening and weakening rules. Moreover, it appears that synapses of later generations, deeply embedded in the network, are pruned with higher probability with respect to bonds of the earlier generations, mostly long range, that mainly support information transmission. Pruning therefore does not affect the small-world property of the Apollonian network. Moreover, the avalanche size distribution shows a power law behavior with an exponent $\sigma=1.8\pm0.2$ for equal and random initial conductances. This value is compatible with 1.5 ± 0.4, experimentally found for neuronal avalanches and recovered by the model on the square-lattice and small-world networks. The avalanche duration distribution exhibits power law behavior with an exponential cutoff, in agreement with experimental results of Beggs and Plentz [2]. The exponent has value $\tau=2.1\pm0.2$ for equal and random initial conductance, in agreement with the value 2.0 found experimentally. Furthermore, the power spectrum exhibits power law behavior at high frequency with $\beta=0.8\pm0.1$, in agreement with experimental data [39,40]. At intermediate frequencies, the slope becomes greater than unity, crossing over to white noise at low frequencies. None of the scaling exponents for the electrical activity in the case of excitatory synapses depends on the particular choice for the length or strength of the plasticity training and are quite stable with respect to the initial conductance configurations. These results suggest that also on Apollonian network universal behavior, found for regular and small world networks [23], holds.

ACKNOWLEDGMENTS

We gratefully thank E. Novikov and collaborators for sharing with us their experimental data. L.d.A. thanks the E.S.P.C.I. in Paris for hospitality. This work was supported by MIUR-PRIN 2004, MIUR-FIRB 2001, CRdC-AMRA, and EU Network Number MRTN-CT-2003-504712. H.J.H. acknowledges support from the Max Planck foundation.

[1] D. Purves *et al.*, *Neuroscience* (Sinauer Associates, Sunderland, MA, 2004).
[2] J. M. Beggs and D. Plenz, J. Neurosci. **23**, 11167 (2003).
[3] J. M. Beggs and D. Plenz, J. Neurosci. **24**, 5216 (2004).
[4] S. Zapperi, K. B. Lauritsen, and H. E. Stanley, Phys. Rev. Lett. **75**, 4071 (1995).
[5] C. W. Eurich, J. M. Herrmann, and U. A. Ernst, Phys. Rev. E **66**, 066137 (2002).
[6] A. Gevins *et al.*, TINS **18**, 429 (1995).
[7] G. Buzsaki and A. Draguhn, Science **304**, 1926 (2004).
[8] J. M. Hausdorff *et al.*, Physica A **302**, 138 (2001).
[9] S. B. Lowen, S. S. Cash, M. Poo, and M. C. Teich, J. Neurosci. **17**, 5666 (1997).
[10] D. R. Chialvo, G. A. Cecchi, and M. O. Magnasco, Phys. Rev. E **61**, 5654 (2000).
[11] P. Bak, *How Nature Works: The science of self-organized criticality* (Springer, New York, 1996).
[12] H. J. Jensen, *Self-Organized Criticality* (Cambridge University Press, Cambridge, England, 1998).
[13] S. Maslov, M. Paczuski, and P. Bak, Phys. Rev. Lett. **73**, 2162 (1994).
[14] J. Davidsen and M. Paczuski, Phys. Rev. E **66**, 050101(R) (2002).
[15] P. Bak and C. Tang, J. Geophys. Res. **94**, 15635 (1989).
[16] A. Sornette and D. Sornette, Europhys. Lett. **9**, 197 (1989).
[17] E. Lippiello, L. de Arcangelis, and C. Godano, Europhys. Lett. **72**, 678 (2005).
[18] P. Bak and K. Sneppen, Phys. Rev. Lett. **71**, 4083 (1993).
[19] E. T. Lu and R. J. Hamilton, Astrophys. J. Lett. **380**, L89 (1991).
[20] P. A. Politzer, Phys. Rev. Lett. **84**, 1192 (2000).
[21] J. Faillettaz, F. Louchet, and J. R. Grasso, Phys. Rev. Lett. **93**, 208001 (2004).
[22] O. Peters, C. Hertlein, and K. Christensen, Phys. Rev. Lett. **88**, 018701 (2002).
[23] L. de Arcangelis, C. Perrone-Capano, and H. J. Herrmann, Phys. Rev. Lett. **96**, 028107 (2006).
[24] T. D. Albraight *et al.*, Neuron **59**, Review Suppl. (2000).
[25] T. K. Hensch, Annu. Rev. Neurosci. **27**, 549 (2004).
[26] L. F. Abbott and S. B. Nelson, Nat. Neurosci. **3**, 1178 (2000).
[27] D. O. Hebb, *The Organization of Behavior* (Wiley, New York, 1949).
[28] J. Z. Tsien, Curr. Opin. Neurobiol. **10**, 266 (2000); G.-Q. Bi and M.-M. Poo, Annu. Rev. Neurosci. **24**, 139 (2001).
[29] S. J. Cooper, Neurosci. Biobehav Rev. **28**, 851 (2005).
[30] O. Shefi, I. Golding, R. Segev, E. Ben-Jacob, and A. Ayali, Phys. Rev. E **66**, 021905 (2002).
[31] D. J. Watts and S. H. Strogatz, Nature (London) **393**, 440 (1998).
[32] L. A. N. Amaral, A. Scala, M. Barthelemy, and E. H. Stanley,

Proc. Natl. Acad. Sci. U.S.A. **97**, 149 (2000).
[33] B. Roerig and B. Chen, Cereb. Cortex **12**, 187 (2002); B. Roerig, B. Chen, and J. P. Y. Kao, *ibid.* **13**, 350 (2003).
[34] C. Wagner and R. Stoop, in *Bifurcation and Chaos*, edited by N. Wessel and J. Kurths; C. Wagner and R. Stoop, in *Bifurcation and Chaos*, edited by S. Boccaletti, 17 (7) (2007).
[35] J. S. Andrade, H. J. Herrmann, R. F. S. Andrade, and L. R. da Silva, Phys. Rev. Lett. **94**, 018702 (2005).
[36] N. S. Desai, J. Physiol. Paris **97**, 391 (2003).
[37] O. Paulsen and T. J. Sejnowski, Curr. Opin. Neurobiol. **10**, 172 (2000).
[38] K. H. Braunewell and D. Manahan-Vaughan, Rev. Neurosci. **12**, 121 (2001).
[39] W. J. Freeman *et al.*, J. Neurosci. Methods **95**, 111 (2000).
[40] E. Novikov, A. Novikov, D. Shannahoff-Khalsa, B. Schwartz, and J. Wright, Phys. Rev. E **56**, R2387 (1997).
[41] J. M. Hausdorff and C. K. Peng, Phys. Rev. E **54**, 2154 (1996).